Photoelectron angular distributions for states of any mixed character: An experiment-friendly model for atomic, molecular, and cluster anions

Dmitry Khuseynov, Christopher C. Blackstone, Lori M. Culberson,[a] and Andrei Sanov[b]
Department of Chemistry and Biochemistry, University of Arizona, Tucson, Arizona 85721, USA

(Received 25 March 2014; accepted 11 September 2014; published online 30 September 2014)

We present a model for laboratory-frame photoelectron angular distributions in direct photodetachment from (in principle) any molecular orbital using linearly polarized light. A transparent mathematical approach is used to generalize the Cooper-Zare central-potential model to anionic states of any mixed character. In the limit of atomic-anion photodetachment, the model reproduces the Cooper-Zare formula. In the case of an initial orbital described as a superposition of *s* and *p*-type functions, the model yields the previously obtained *s*-*p* mixing formula. The formalism is further advanced using the Hanstorp approximation, whereas the relative scaling of the partial-wave cross-sections is assumed to follow the Wigner threshold law. The resulting model describes the energy dependence of photoelectron anisotropy for any atomic, molecular, or cluster anions, usually without requiring a direct calculation of the transition dipole matrix elements. As a benchmark case, we apply the *p*-*d* variant of the model to the experimental results for NO^- photodetachment and show that the observed anisotropy trend is described well using physically meaningful values of the model parameters. Overall, the presented formalism delivers insight into the photodetachment process and affords a new quantitative strategy for analyzing the photoelectron angular distributions and characterizing mixed-character molecular orbitals using photoelectron imaging spectroscopy of negative ions. © *2014 AIP Publishing LLC*. [http://dx.doi.org/10.1063/1.4896241]

I. INTRODUCTION

Photoelectron imaging spectroscopy is a versatile technique for probing the electronic structure of atoms and molecules. The corresponding spectra contain information about the electronic, vibrational, and possibly even rotational energy levels of the species studied.[1] The photoelectron angular distributions (PADs), which can be measured in various contexts,[2] reflect the geometric properties of the parent orbitals, closely related to differential photodetachment cross-sections.[3]

In the particular case of one-photon laboratory-frame measurements, the orientation averaging takes a toll on the observables, but the relative ease of the experiments opens a door for extensive investigations of a broad range of systems. As molecules increase in size, the PADs may become less anisotropic, but this trend itself, if analyzed properly, can shed light on the increasing structural complexity. With a particular focus on anion photodetachment, one broad objective of this article is to help refute the perception that the information content of one-photon laboratory-frame PADs automatically and necessarily diminishes with increasing complexity of the systems studied. We discuss, in conceptual and quantitative detail, how the general mixed (hybrid) character of molecular orbitals is reflected in the corresponding PADs. The experiment-friendly approach to modeling the PADs is hoped to propel future applications of photoelectron imaging to more routine characterizations of complex mixed-character orbitals. In a related realm, the analysis of PADs for known systems, within the model framework presented here, will solidify the conceptual and pedagogical connection of photodetachment physics with chemistry, as manifest in the molecular bonding structures.

The laboratory-frame PADs in one-photon detachment (or ionization) using linearly polarized light are given, in general, by[4]

$$\sigma'(\theta) = (\sigma/4\pi)[1 + \beta P_2(\cos\theta)], \tag{1}$$

where θ is the angle between the photoelectron velocity vector and the light's electric field vector, $P_2(\cos\theta) = (1/2)(3\cos^2\theta - 1)$ is the second-order Legendre polynomial, σ is the total (integrated) photodetachment cross-section, $\sigma' \equiv d\sigma/d\Omega$ is the differential cross-section with respect to the solid angle Ω ($d\Omega = \sin\theta d\theta$), and β is the anisotropy parameter, ranging from -1 to 2 for purely perpendicular and parallel transitions, respectively.

In the case of atomic species, the initial state of the electron can usually be described, within the orbital approximation, by a definite value of the orbital angular momentum quantum number, l. Due to the angular momentum conservation, the electrons emitted in a one-photon detachment or ionization process are represented by superposition of partial waves with quantum numbers $l \pm 1$. According to the derivations by Bethe,[5] generalized by Cooper and Zare,[6,7] the anisotropy parameter β for atomic ionization or photodetachment is given by the following expression, commonly referred to as the Cooper-Zare central-potential formula:

[a]Present address: Sandia National Laboratories, MS 9055, Livermore, California 94551, USA.
[b]E-mail: sanov@u.arizona.edu.

$$\beta_l = \frac{l(l-1)\chi^2_{l,l-1} + (l+1)(l+2)\chi^2_{l,l+1} - 6l(l+1)\chi_{l,l+1}\chi_{l,l-1}\cos\delta_{l+1,l-1}}{(2l+1)\left[l\,\chi^2_{l,l-1} + (l+1)\chi^2_{l,l+1}\right]}. \quad (2)$$

In this equation, $\chi_{l,l\pm1}$ are the magnitudes of the radial transition dipole matrix elements for the $(l \pm 1)$ partial waves originating from the initial atomic orbital with the orbital angular momentum quantum number l and $\delta_{l+1,l-1}$ is the corresponding phase shift induced by interactions with the remaining neutral or ion.

Equation (2) is generally not applicable to molecular or cluster species, for which l is not defined.[8,9] In some cases, however, when the molecular orbital (MO) resembles an atomic-like function, an effective-l description may be adopted. For example, the $2p\pi_g{}^*$ highest-occupied MO (HOMO) of $O_2{}^-$ is a d-like function, hence the photodetachment of $O_2{}^-$ can be modeled approximately using the central-potential model with $l = 2$.[10–12] As another example, photodetachment[13,14] from CH^- effectively involves the nonbonding $2p$ orbitals of the carbon atom and can be modeled with the Cooper-Zare formula with $l = 1$.[15] As most MOs cannot be described by a single l value, many attempts have been made to develop a general Cooper-Zare-like equation for molecular species.[16–21] One such development is the theory for PADs of diatomic molecules by Buckingham *et al.*,[20,21] discussed in Sec. II D of this work. Unfortunately, none of the previous formulations can be viewed as both general and straightforward.

As the direct precursor to the present work, our group has recently developed an analogue of the Cooper-Zare formula for photodetachment from mixed s-p orbitals.[22–24] Although the approach used to derive the model is general (at least in principle),[23] the mixed s-p formula itself is not. Specifically, it assumes that the initial state of the electron is a linear combination of one s and one p type functions localized on the same center:[23,24]

$$|\psi_{sp}\rangle = \sqrt{1-\gamma_p}|s\rangle + \sqrt{\gamma_p}|p\rangle, \quad (3)$$

where γ_p is the fractional p character, $0 \le \gamma_p \le 1$. [Originally, f (for fractional) was used in Eq. (3) instead of γ_p.[3,22–25] Here, we change the notation to make it amendable to any general mixing case, including those with f orbital contributions.] Any relative phase factors for the s and p components in Eq. (3) are absorbed into the corresponding kets. The key equation of the mixed s-p model, expressed in the form analogous to Eq. (2), is

$$\beta_{sp} = \frac{2(1-\gamma_p)\chi^2_{0,1} + \gamma_p\left(2\chi^2_{1,2} - 4\chi_{1,0}\chi_{1,2}\cos\delta_{2,0}\right)}{(1-\gamma_p)\chi^2_{0,1} + \gamma_p\left(\chi^2_{1,0} + 2\chi^2_{1,2}\right)}. \quad (4)$$

Although it does not contain l explicitly, the l values for the s and p components of the initial orbital have been assumed in the derivation of the model.[22,23] Although the Cooper-Zare formula was not used in the derivation, in the limiting cases of a pure s ($\gamma_p = 0$) and pure p ($\gamma_p = 1$) orbitals, Eq. (4) reduces exactly to the corresponding Cooper-Zare predictions, i.e., Eq. (2) with $l = 0$ and $l = 1$, respectively. With additional approximations,[26] the mixed s-p model has been shown to predict correctly the behavior of the anisotropy parameter with respect to electron kinetic energy (eKE) for several polyatomic anions, particularly those with hybrid sp^n orbitals.[25,27] It also performs well for atomic and atomic-like anions perturbed by cluster solvation.[23,28]

In general, any MO can be formally represented as a combination of atomic-orbital functions centered at a chosen point in space. This is the central idea of this work. The specific objective is to generalize the Cooper-Zare central-potential model,[5–7] as well as the mixed s-p model,[23] to molecular or cluster states of any mixed character. We develop a transparent mathematical approach, which allows one to construct an analogous expression for the photodetachment from any MO. We use the same assumptions as those underlying the Cooper-Zare central-potential model, but do not use the Cooper-Zare formula explicitly. Instead, we show that in the limiting cases of atomic anions the Cooper-Zare formula naturally follows from the present work. The present approach also differs from the original derivation of the mixed s-p model by Grumbling *et al.*:[22,23] while the original formulation considered only the so-called principal molecular orientations, instead of complete orientation averaging, no such approximation is used here.

Section II presents the general model formalism and first considers its application to s-p mixing, as a test case for comparison with the previous formulation.[22,23] We confirm that the previous approach yielded the same s-p mixing result, which follows from the more general model described here. We then follow through with an analogous derivation for the p-d mixing case and subsequently introduce a general expression for photoelectron anisotropy for any mixed MO. In Sec. III, we employ additional approximations and develop a more practical adaptation of the model to describe the explicit eKE dependence of the anisotropy parameter. Section IV considers the photodetachment of NO^- as a benchmark case for the p-d mixing variant of the theory.

II. GENERALIZED MIXING MODEL

The differential cross-sections for one-photon detachment can be calculated through the corresponding transition dipole matrix elements $\vec{\mu}_{fi}$, by integrating the magnitude-squared of the scalar product of $\vec{\mu}_{fi}$ and light's electric field vector with respect to all molecular orientations.[5,29] The calculation of $\vec{\mu}_{fi}$ requires the knowledge of the parent MO (or its Dyson analogue[30]) and the outgoing electron wave. Essentially, one starts from an assumed initial state, defined in the molecular frame, and projects it (with the dipole operator) on the final state interrogated in the laboratory frame.

We approach the same process from the final-state perspective, starting with a formal expansion of the photoelectron

wave in the complete symmetry-adapted laboratory-frame basis of spherical harmonics integrated over the azimuth angle, $\Theta_{l,m}(\theta)$. The differential cross-section may then be represented as a sum over the angular-momentum components of the free electrons:

$$\sigma'(\theta) = N\left|\sum_{l=0}^{\infty}\sum_{m=-l}^{l} C_{\ell,m}\Theta_{\ell,m}(\theta)\right|^2 = N\sum_{l=0}^{\infty}\sum_{l'=0}^{\infty}\sum_{m=-l}^{l}\sum_{m'=-l'}^{l'} C_{\ell,m}C^*_{\ell',m'}\Theta_{\ell,m}(\theta)\Theta^*_{\ell',m'}(\theta), \tag{5}$$

where N is a normalization-dependent pre-factor. The energy (or linear momentum) dependent $C_{l,m}$ coefficients in Eq. (5) define the amplitudes of the partial waves and hence the partial differential cross-sections, as observed in the laboratory frame. To this point, the quadruple-sum in Eq. (5) is similar to Eq. (20) in Ref. 31, where Oana and Krylov calculated the differential cross-sections by explicitly averaging the contributions of all molecular orientations. Despite the revealing similarity, Eq. (5) is in no way dependent on the details of orientation averaging. It follows directly from the formal expansion of the free-electron wavefunction (defined by the double sum in the first part of the equation) in the complete laboratory frame basis.[3] This expansion is mathematical in nature and may be written for any photodetachment process – atomic or molecular – without explicit reference to the parent orbitals or orientation averaging. The $C_{l,m}$ coefficients are defined in the laboratory frame, where the final state of the detached electron is observed. The treatment of the orientation averaging, along with the knowledge of the bound orbitals, is necessary for the explicit evaluation of the coefficients, but not for the formal statement of Eq. (5). In what follows, we show that physical insight may be obtained using a simplified treatment of this expansion.

As follows from Eq. (1), the complete $\sigma'(\theta)$ function in Eq. (5) is not required for the calculation of β. It is sufficient to know the relative cross-sections for just two angles, e.g., $\theta = 0$ and $\theta = \pi/2$:

$$\beta = \frac{2\left(\sigma'(0) - \sigma'(\pi/2)\right)}{\sigma'(0) + 2\sigma'(\pi/2)}. \tag{6}$$

This realization simplifies the following derivation, as many of the spherical harmonics in Eq. (5) vanish at these angles.

A. Photodetachment from orbitals with definite *l* values

In this subsection, we derive the expressions for the differential cross-sections at $\theta = 0$ and $\pi/2$ that will be used in Sec. II B in conjunction with in Eq. (6) for anisotropy parameter calculations. First, we consider photodetachment from a p orbital ($l = 1$, $m = 0, \pm 1$), as the simplest case where the PAD is dictated by nontrivial partial-wave interference. The analogous derivations for s and d orbitals are presented in Part A of the supplementary material,[32] with only the key results summarized here, in the body of the article.

According to the selection rules $\Delta l = \pm 1$, $\Delta m = 0$ (linearly polarized light), the outgoing waves in p orbital photodetachment are described by the harmonics $\Theta_{0,0}(\theta)$, $\Theta_{2,0}(\theta)$, and $\Theta_{2,\pm1}(\theta)$. At $\theta = 0$ and $\pi/2$, $\Theta_{2,\pm1} = 0$; hence, the corresponding waves do not contribute to the ejection of photoelectrons at 0° and 90°. Therefore, for these two angles *only*, Eq. (5) takes the form:

$$\sigma'_p(\theta) = N\big(C^2_{0,0}\Theta^2_{0,0}(\theta) + 2C_{0,0}C_{2,0}\cos\delta_{2,0}\Theta_{0,0}(\theta)\Theta_{2,0}(\theta) + C^2_{2,0}\Theta^2_{2,0}(\theta)\big), \tag{7}$$

assuming (for brevity and simplicity) that all $C_{l,m}$ coefficients are real. Throughout this work, σ'_l, $l = 0, 1, 2, \ldots$ or $s, p, d, \ldots$, denotes the differential cross-section for detachment from an l orbital, accounting for the interference of the $(l \pm 1)$ partial waves. Substituting $\Theta_{0,0}(\theta) = \frac{1}{2\sqrt{\pi}}$ and $\Theta_{2,0}(\theta) = \frac{1}{4}\sqrt{\frac{5}{\pi}}(3\cos^2\theta - 1)$ into Eq. (7), we obtain

$$\sigma'_p(\theta) = \frac{N}{4\pi}\left(C^2_{0,0} + \sqrt{5}C_{0,0}C_{2,0}\cos\delta_{2,0}(3\cos^2\theta - 1) + \frac{5}{4}C^2_{2,0}(3\cos^2\theta - 1)^2\right). \tag{8}$$

Although this equation is valid only for $\theta = 0$ and $\theta = \pi/2$, it is sufficient for our purpose. Substituting (sequentially) $\theta = 0$ and $\theta = \pi/2$ into Eq. (8) and using the results in Eq. (6), we obtain the following expression for the anisotropy parameter in p orbital photodetachment:

$$\beta_p = \frac{\frac{15}{8\pi}C^2_{2,0} + \frac{3\sqrt{5}}{2\pi}C_{0,0}C_{2,0}\cos\delta_{2,0}}{\frac{3}{4\pi}C^2_{0,0} + \frac{15}{8\pi}C^2_{2,0}}. \tag{9}$$

Even though only $\theta = 0$ and $\pi/2$ were used to arrive at this result, it defines the entire PAD ($\theta = 0$ to π) through Eq. (1). In general, the $C_{l,m}$ coefficients in Eq. (5) – and therefore Eq. (9) – are related to the $\chi_{l,l\pm1}$ matrix elements in Eq. (2). For the purpose of this work, it is sufficient and easiest to deduce this relationship indirectly, using the approach described in Ref. 31. Specifically, we compare Eq. (9) to the corresponding Cooper-Zare expression, i.e., Eq. (2) with $l = 1$:

$$\beta_p = \frac{2\chi^2_{1,2} - 4\chi_{1,0}\chi_{1,2}\cos\delta_{2,0}}{\chi^2_{1,0} + 2\chi^2_{1,2}}. \tag{10}$$

Since Eqs. (9) and (10) describe the same physics, they must be identical. We hence arrive at the proportionality $C_{2,0}/C_{0,0} = -(2/\sqrt{5})\,\chi_{1,2}/\chi_{1,0}$, which we re-write, for convenience, as a system of two equations with a common coefficient M_1 (the subscript indicates $l = 1$ for a p orbital):

$$\begin{cases} C_{0,0} = -2M_1\sqrt{\pi}\chi_{1,0} \\ C_{2,0} = 4M_1\frac{\sqrt{\pi}}{\sqrt{5}}\chi_{1,2} \end{cases}. \tag{11}$$

Substituting Eq. (11) into Eq. (8), we obtain the expressions for the differential cross-section at $\theta = 0$ and $\theta = \pi/2$ in the detachment from a p orbital:

$$\begin{cases} \sigma'_p(0) = M_1^2 N\left(\chi_{1,0}^2 + 4\chi_{1,2}^2 - 4\chi_{1,0}\chi_{1,2}\cos\delta_{2,0}\right) \\ \sigma'_p(\pi/2) = M_1^2 N\left(\chi_{1,0}^2 + \chi_{1,2}^2 + 2\chi_{1,0}\chi_{1,2}\cos\delta_{2,0}\right) \end{cases}. \quad (12)$$

As a matter of verification, substituting Eq. (12) into Eq. (6) yields Eq. (10), i.e., the Cooper-Zare expression for p orbital photodetachment.

Analogous derivations can be repeated for any parent orbital with a definite l value. The specific cases of s and d orbitals are detailed in Part A of the supplementary material.[32] Here, we summarize the results that will be used in the subsequent discussion.

In the trivial case of detachment from an s orbital ($l = 0$, $m = 0$), only the $\Theta_{1,0}$ wave is emitted and the differential cross-section magnitudes at $\theta = 0$ and $\theta = \pi/2$ are given by[32]

$$\begin{cases} \sigma'_s(0) = M_0^2 N \chi_{0,1}^2 \\ \sigma'_s(\pi/2) = 0 \end{cases}. \quad (13)$$

The analysis becomes progressively more complex for larger values of l. For a d orbital ($l = 2$, $m = 0, \pm1, \pm2$), there are eight outgoing waves, described by the harmonics $\Theta_{1,0}(\theta)$, $\Theta_{1,\pm1}(\theta)$, $\Theta_{3,0}(\theta)$, $\Theta_{3,\pm1}(\theta)$, and $\Theta_{3,\pm2}(\theta)$. Although $\Theta_{3,\pm2}(\theta)$ vanish for $\theta = 0$ and $\theta = \pi/2$ and, therefore, do not contribute to photoemission in these directions, the remaining harmonics still result in 21 terms that must be considered in Eq. (5). The final result is[32]

$$\begin{cases} \sigma'_d(0) = M_2^2 N\left(4\chi_{2,1}^2 + 9\chi_{2,3}^2 - 12\chi_{2,1}\chi_{2,3}\cos\delta_{3,1}\right) \\ \sigma'_d(\pi/2) = M_2^2 N\left(3\chi_{2,1}^2 + 3\chi_{2,3}^2 + 6\chi_{2,1}\chi_{2,3}\cos\delta_{3,1}\right) \end{cases}. \quad (14)$$

The differential cross-sections for higher-order atomic orbitals are not considered explicitly in this work, but their magnitudes for $\theta = 0$ and $\theta = \pi/2$ can be derived (with some patience) following the procedure detailed here.

B. Photodetachment from mixed-character states

The derivations in Sec. II A were performed for atomic orbitals. Upon substitution into Eq. (6), they yield the Cooper-Zare formulae for the corresponding l values. We now show that the differential cross-sections for $\theta = 0$ and $\theta = \pi/2$, expressed as explicit functions of the corresponding radial dipole elements $\chi_{l,l\pm1}$, lead to a straightforward method for constructing the formulae for the anisotropy parameter in the detachment from *any* mixed state. We begin with a re-derivation of the mixed s-p model, obtained previously using a different approach.[3,22–24] This will serve as an initial test of the generalized mixing theory presented below.

In calculations of cross-sections, one sums over the final states, but averages over the degenerate initial states. For a mixed s-p state described by Eq. (3), the differential cross-sections can thus be shown to be the weighted average of the contributions of the s and p components of the initial state:

$$\sigma'_{sp}(\theta) = (1 - \gamma_p)\,\sigma'_s(\theta) + \gamma_p\,\sigma'_p(\theta). \quad (15)$$

In this expression, interference between the $p \to s$ and $p \to d$ channels is included in $\sigma_p{}'$, per Eq. (7), while the cross-terms for the $s \to p$ and $p \to s$, as well as $s \to p$ and $p \to d$ channels are zeroed out by orientation averaging, as discussed previously.[23] Substituting Eqs. (13) and (12) into Eq. (15) yields:

$$\begin{cases} \sigma'_{sp}(0) = M_0^2 N(1-\gamma_p)\chi_{0,1}^2 + M_1^2 N\gamma_p\left(\chi_{1,0}^2 + 4\chi_{1,2}^2 - 4\chi_{1,0}\chi_{1,2}\cos\delta_{2,0}\right) \\ \sigma'_{sp}(\pi/2) = M_1^2 N\gamma_p\left(\chi_{1,0}^2 + \chi_{1,2}^2 + 2\chi_{1,0}\chi_{1,2}\cos\delta_{2,0}\right). \end{cases} \quad (16)$$

Upon substitution of Eq. (16) into Eq. (6), we obtain

$$\beta_{sp} = \frac{2M_0^2 N(1-\gamma_p)\chi_{0,1}^2 + 2M_1^2 N\gamma_p\left(3\chi_{1,2}^2 - 6\chi_{1,0}\chi_{1,2}\cos\delta_{2,0}\right)}{M_0^2 N(1-\gamma_p)\chi_{0,1}^2 + M_1^2 N\gamma_p\left(3\chi_{1,0}^2 + 6\chi_{1,2}^2\right)}. \quad (17)$$

While the N coefficient in Eq. (17) cancels out, M_0 and M_1 do not. In general, M_l depends on l, for the following reason. The differential and total cross-sections, which are proportional to ${M_l}^2$, include a sum over all final states and an average over the $(2l + 1)$ degenerate initial states. Thus, both $\sigma_l{}'$ and σ_l must be proportional to the dipole elements squared, divided by $(2l + 1)$.[21] Hence, ${M_l}^2 \propto (2l + 1)^{-1}$, which can be expressed as ${M_l}^2 = M^2/(2l + 1)$, where M is a factor independent of l. It follows then that ${M_0}^2 = 3{M_1}^2$. Using this proportionality in Eq. (17) yields the familiar s-p mixing formula, Eq. (4). Previously, Eq. (4) was obtained by analyzing the geometric properties of the relevant partial waves emitted from three "principal orientations" of the anion.[23] The agreement of the new derivation with the previous result is an important validation point.

A similar procedure can be applied to a superposition of p and d orbitals,

$$|\psi_{pd}\rangle = \sqrt{1-\gamma_d}|p\rangle + \sqrt{\gamma_d}|d\rangle, \quad (18)$$

where γ_d is the fractional d character. Using the p-d analogue of Eq. (15) and referring to Eqs. (6), (12), (14), and $M_l^2 = M^2/(2l+1)$, we obtain the anisotropy parameter for mixed p-d state photodetachment:

$$\beta_{pd} = \frac{(1-\gamma_d)\left(2\chi_{1,2}^2 - 4\chi_{1,0}\chi_{1,2}\cos\delta_{2,0}\right) + \gamma_d\left(2\chi_{2,1}^2 + 12\chi_{2,3}^2 - 36\chi_{2,1}\chi_{2,3}\cos\delta_{3,1}\right)/5}{(1-\gamma_d)\left(\chi_{1,0}^2 + 2\chi_{1,2}^2\right) + \gamma_d\left(2\chi_{2,1}^2 + 3\chi_{2,3}^2\right)}. \tag{19}$$

In the limiting cases of $\gamma_d = 0$ and $\gamma_d = 1$, Eq. (19) reduces exactly to the Cooper-Zare predictions for the detachment from pure p and pure d states, i.e., Eq. (2) with $l = 1$ and $l = 2$, respectively. This property of Eq. (19) is similar to that of Eq. (4) for s-p mixing.

The above approach allows us to construct analogous expressions for the detachment from *any* mixed orbital, and therefore, at least in principle, from anything or everything. It can be easily generalized for any number of different l components, not necessarily just one [as in the Cooper-Zare formula, Eq. (2)] or two (as in the s-p and p-d mixing cases discussed above).

Since atomic orbitals localized on a single center form a complete basis set, any MO can be expanded as their linear combination.[3] We assume

$$|\psi_{\mathrm{MO}}\rangle = \sum_l \sqrt{\gamma_l}|l\rangle, \tag{20}$$

where $|l\rangle$ are suitable linear combinations of orbitals of a given type (defined l value and $m = -l \ldots l$), adapted to the system at hand. The phase factors are absorbed into the kets, while γ_l are the fractional l characters ($l = s$, p, d, etc.) that satisfy the normalization requirement $\sum_l \gamma_l = 1$. Equation (20) is expressed in this particular form, because the projection of angular momentum on a given axis (described by the quantum number m) is not conserved upon the molecular-to-laboratory frame transformation for a randomly oriented ensemble, but the angular momentum magnitude (described by l) is conserved. Hence, for modeling the laboratory-frame PADs the l composition of the parent MO, not its m distribution, is important. Generalizing the approach used to obtain the s-p and p-d mixing formulae [Eqs. (4) and (19)], the anisotropy parameter for the detachment from the mixed orbital defined by Eq. (20) is given by

$$\beta = \frac{\sum_l \gamma_l\left[l(l-1)\chi_{l,l-1}^2 + (l+1)(l+2)\chi_{l,l+1}^2 - 6l(l+1)\chi_{l,l-1}\chi_{l,l+1}\cos\delta_{l+1,l-1}\right]/(2l+1)}{\sum_l \gamma_l\left[l\chi_{l,l-1}^2 + (l+1)\chi_{l,l+1}^2\right]}. \tag{21}$$

In general, the expansion in Eq. (20) may contain an infinite number of terms. Its convergence, and hence the number of mixing terms needed under the sums in Eq. (21), depend on the basis set. For practical applications, the basis can be (should be) chosen carefully, to limit the number of terms, while maximizing physical insight over computational rigor. Many striking applications can be demonstrated with just two basis functions, giving rise to the special "binary" mixing cases. The mixed s-p model[22–24] is the very first such example, the next being the p-d mixing case, whose application is discussed in Sec. IV.

C. Simple empirical rule for MOs of any mixed character

Equation (21) allows us to formulate a simple empirical rule for writing the Cooper-Zare-like equation for any specific mixing case.

First, it is convenient to express the Cooper-Zare formula,[6,7] Eq. (2), as a ratio:

$$\beta_l = v_l/w_l, \tag{22}$$

where

$$v_l = \frac{l(l-1)\chi_{l,l-1}^2 + (l+1)(l+2)\chi_{l,l+1}^2 - 6l(l+1)\chi_{l,l-1}\chi_{l,l+1}\cos\delta_{l+1,l-1}}{2l+1},$$
$$w_l = l\chi_{l,l-1}^2 + (l+1)\chi_{l,l+1}^2. \tag{23}$$

We shall refer to v_l and w_l as the Cooper-Zare numerator and denominator, respectively, despite the fact that the $(2l+1)$ divider in v_l is usually written in the denominator of the Cooper-Zare formula.[6,7] The denominator w_l is related to the photodetachment cross-section σ_l, via $\sigma_l \propto (2l+1)^{-1} w_l$,[20,21] with the $(2l+1)^{-1}$ factor accounting for the averaging over the degenerate states with quantum number l. It is for this reason that in Sichel's work[21] the Cooper-Zare formula is written with $(2l+1)^{-1}$ in the denominator, offset by $(2l+1)^{-2}$

in the numerator, in contrast to the more common format of Eq. (2),[6,7] which has a $(2l+1)$ factor in the denominator only.

Using Eq. (23), the *s-p* mixing formula, Eq. (4), may be written compactly as

$$\beta_{sp} = \frac{(1-\gamma_p)v_0 + \gamma_p v_1}{(1-\gamma_p)w_0 + \gamma_p w_1}. \tag{24}$$

The *p-d* mixing formula, Eq. (19), can be expressed in a similar form:

$$\beta_{pd} = \frac{(1-\gamma_d)v_1 + \gamma_d v_2}{(1-\gamma_d)w_1 + \gamma_d w_2}. \tag{25}$$

Comparing the general mixing formula, Eq. (21), to the definitions in Eq. (23), the former may be written simply as

$$\beta = \frac{\sum_l \gamma_l v_l}{\sum_l \gamma_l w_l}. \tag{26}$$

Hence, Eq. (21) is but a ratio of the Cooper-Zare numerators and denominators, individually averaged over all l components of the parent MO with the respective fractional characters γ_l. When "mixing" the respective Cooper-Zare numerators and denominators in such an empirical way, the $(2l+1)$ degeneracy factor (commonly appearing in the denominator of the Cooper-Zare formula)[6,7] must be treated as part of the numerator, per Eq. (23).

For example, the Cooper-Zare formulae for pure *s* and *p* orbitals are given by Eq. (S.2) in the supplementary material[32] and Eq. (10) above, respectively. Mixing (averaging) the respective numerators, $v_0 = 2\chi_{0,1}^2$ and $v_1 = (2\chi_{1,2}^2 - 4\chi_{1,0}\chi_{1,2}\cos\delta_{2,0})$, and denominators, $w_0 = \chi_{0,1}^2$ and $w_1 = (\chi_{1,0}^2 + 2\chi_{1,2}^2)$, using $(1-\gamma_p)$ and γ_p for the *s* and *p* fractional characters, yields the *s-p* mixing equation, Eq. (4). We have thus obtained the *s-p* mixing result in an empirical fashion, without going through the intermediate derivation steps described earlier in this section or in Ref. 23.

Turning to *p-d* mixing, the Cooper-Zare formula for detachment from a *p* orbital is given by Eq. (10), with the numerator v_1 and denominator w_1 appearing in the preceding paragraph. The analogous expression for a *d* orbital is obtained by substituting $l = 2$ into Eq. (2):

$$\beta_d = \frac{\left(2\chi_{2,1}^2 + 12\chi_{2,3}^2 - 36\chi_{2,1}\chi_{2,3}\cos\delta_{3,1}\right)/5}{2\chi_{2,1}^2 + 3\chi_{2,2}^2}, \tag{27}$$

i.e., $v_2 = (2\chi_{2,1}^2 + 12\chi_{2,3}^2 - 36\chi_{2,1}\chi_{2,3}\cos\delta_{3,1})/5$ and $w_2 = 2\chi_{2,1}^2 + 3\chi_{2,2}^2$. Using $(1-\gamma_d)$ and γ_d for the *p* and *d* characters, respectively, yields the *p-d* mixing equation, Eq. (19), also skipping all the intermediate steps described in Sec. II B and in Part A of the supplementary material.[32]

As another illustration of the empirical approach, we shall write the anisotropy equation for detachment from a mixed *d-f* state with a fractional *f* character γ_f, avoiding the exceedingly tedious derivation altogether. Since the Cooper-Zare formula for a *d* orbital is given by Eq. (27), while that for an *f* orbital [substituting $l = 3$ into Eq. (2)] is

$$\beta_f = \frac{\left(6\chi_{3,2}^2 + 20\chi_{3,4}^2 - 72\chi_{3,2}\chi_{3,4}\cos\delta_{4,2}\right)/7}{3\chi_{3,2}^2 + 4\chi_{3,4}^2}, \tag{28}$$

the above procedure yields the formal *d-f* mixing result in one simple step:

$$\beta_{df} = \frac{(1-\gamma_f)\left(2\chi_{2,1}^2 + 12\chi_{2,3}^2 - 36\chi_{2,1}\chi_{2,3}\cos\delta_{3,1}\right)/5 + \gamma_f\left(6\chi_{3,2}^2 + 20\chi_{3,4}^2 - 72\chi_{3,2}\chi_{3,4}\cos\delta_{4,2}\right)/7}{(1-\gamma_f)\left(2\chi_{2,1}^2 + 3\chi_{2,3}^2\right) + \gamma_f\left(3\chi_{3,2}^2 + 4\chi_{3,4}^2\right)}. \tag{29}$$

Analogous equations can be similarly formulated for any other mixing scenario, including cases of more than two types of functions contributing to the MO expansion in Eq. (20).

D. Comparison to Buckingham *et al.*'s theory for diatomics

Before continuing with the practical adaptation of the generalized mixing theory, we discuss the results obtained so far in the context of Buckingham *et al.*'s theory for PADs of diatomic molecules.[20,21] The bulk of their work accounts for rotational structure within different angular-momentum coupling cases. They showed, however, [Eq. (30) in Ref. 20] that in the absence of rotational resolution (averaging over the rotational levels), the photoelectron anisotropy parameter for a linear molecule is given by (adapting the notation to that used in the present work)

$$\beta = \frac{\sum_{l=|\Delta\Lambda|}^{\infty} |c_{nl}|^2 (2l+1)^{-2}\left[l(l-1)\chi_{l,l-1}^2 + (l+1)(l+2)\chi_{l,l+1}^2 - 6l(l+1)\chi_{l,l-1}\chi_{l,l+1}\cos\delta_{l+1,l-1}\right]}{\sum_{l=|\Delta\Lambda|}^{\infty} |c_{nl}|^2 (2l+1)^{-1}\left[l\chi_{l,l-1}^2 + (l+1)\chi_{l,l+1}^2\right]}, \tag{30}$$

where c_{nl} are the parent MO expansion coefficients with respect to the central-potential basis and $\Delta\Lambda$ is the change in the projection of the electronic orbital angular momentum on the internuclear axis due to the photoionization or photodetachment transition. Within the MO approximation, $\Delta\Lambda$ corresponds to the projection of angular momentum of the parent orbital (λ). For a single l value, Eq. (30) reduces to the corresponding Cooper-Zare formula, Eq. (2).

There is revealing similarity between the general mixing equation, Eq. (21), and Buckingham *et al.*'s[20] rotation-averaged result for diatomic molecules, Eq. (30). To emphasize this point, Eq. (30) may be rewritten in the following form, using the definitions of Eq. (23):

$$\beta = \frac{\sum_{l=|\Delta\Lambda|}^{\infty} |c_{nl}|^2 (2l+1)^{-1} v_l}{\sum_{l=|\Delta\Lambda|}^{\infty} |c_{nl}|^2 (2l+1)^{-1} w_l}. \tag{31}$$

This equation is similar to the general mixing formula obtained here, in the form of Eq. (26), with two distinctions.

First, the weight factors under the sums are different, but easily reconciled. The $|c_{nl}|^2$ coefficients in Eq. (30) or (31) represent the weights of different l components of the initial MO. In Eq. (21) or, equivalently, Eq. (26) these weights are expressed in the equivalent form of fractional l character, γ_l. Further, the $(2l+1)$ dividers in Eq. (31) account for the averaging over the m_l components of the degenerate states with defined l values.[20] Similar factors do not appear in Eq. (26), because of how the initial state is defined in our derivation, per Eq. (20). For example, in the *s*-*p* mixing variant of the model, the initial state is defined as a superposition of one *s*- and one *p*-type function, while other *m* components of the *p* state do not contribute to the detachment MO. All necessary averaging is hence accounted for by γ_p in Eq. (3) or, generally, γ_l in Eq. (20).

The second distinction between Eqs. (26) and (31) is the respective summation ranges. In Eq. (26), we sum (average) over all l components of the initial MO included in the consideration. In Eq. (31), the sum starts, effectively, at $l = |\lambda|$, where λ is the projection of l of the parent MO on the linear molecule's axis. Hence, this distinction reflects the different scopes of applicability of the two models (polyatomics vs. linear molecules), while the conceptual foundation behind the basis-set expansions is the same in both cases.

Overall, the approach taken in the present work is distinct from that used by Buckingham *et al.*[20,21] In Secs. II A–II C, the averaging over the rotational structure is included implicitly, rather than explicitly. The disregard of rotational structure leads to the loss of the corresponding observables but has also resulted in tremendous simplifications in the formalism, allowing it to be extended to any polyatomic system. Yet, in the partial case of diatomics the final result coincides with Buckingham *et al.*'s[20] rotation-averaged formula, giving an important validation to our theory.

III. THE HANSTORP APPROXIMATION

A. Application to the central-potential and *s*-*p* mixing models

The direct application of the Cooper-Zare model,[6,7] the generalized mixing theory (Secs. II A–II C), or the theory of Buckingham *et al.*[20,21] (Sec. II(D)) requires the evaluation of the energy-dependent transition matrix elements, $\chi_{l,l\pm1}$. That being a nontrivial undertaking in its own right,[10] the PADs for relatively simple species, in conjunction with the Cooper-Zare model, are sometimes used to deduce these quantities from experimental data.

For applications relevant to chemistry, it is often desirable to decouple the matrix elements problem from the underlying properties of the MOs themselves. This objective can be achieved via an alternative approach, applicable only to anion photodetachment, which is based on the approximation originally proposed by Hanstorp and co-workers.[26] They assumed that the relative scaling of the partial-wave cross-sections and, therefore, the transition dipole matrix elements follows the Wigner law.[33] The Cooper-Zare formula, Eq. (2), can be rearranged to show that β_l is dependent not on the matrix elements themselves but the $\chi_{l,l+1}/\chi_{l,l-1}$ ratio. Assuming the ratio of the $(l+1)$ and $(l-1)$ partial wave cross-sections to be proportional to ε^2, where $\varepsilon \equiv$ eKE, and, therefore, $\chi_{l,l+1}/\chi_{l,l-1} = A_l\varepsilon$, where A_l is a proportionality coefficient, Eq. (2) can be rearranged to allow the calculation of β_l as an explicit function of eKE:[26]

$$\beta_l(\varepsilon) = \frac{l(l-1) + (l+1)(l+2)A_l^2\varepsilon^2 - 6l(l+1)A_l\varepsilon\cos\delta_{l+1,l-1}}{(2l+1)\left[l + (l+1)A_l^2\varepsilon^2\right]}. \tag{32}$$

In a similar vein, all applications of the *s*-*p* mixing model published to date[3,14,23–25,27] have used the Hanstorp-like[26] form of Eq. (4), namely[23,24]

$$\beta_{sp}(\varepsilon) = \frac{2(1-\gamma_p)B_1\varepsilon + \gamma_p\left(2A_1^2\varepsilon^2 - 4A_1\varepsilon\cos\delta_{2,0}\right)}{(1-\gamma_p)B_1\varepsilon + \gamma_p\left(1 + 2A_1^2\varepsilon^2\right)}. \tag{33}$$

Equation (33) gives the explicit eKE dependence of the anisotropy parameter in a manner analogous to Eq. (32) for defined-l states. The A_1 coefficient in Eq. (33) describes the relative scaling of the $p \to d$ and $p \to s$ detachment channels; it is but a specific ($l = 1$) case of A_l used in Eq. (32), which describes the same for the $l \to l \pm 1$ channels originating from the initial l orbital. The B_1 coefficient in Eq. (33) was first introduced (originally as simply B) in the *s*-*p* mixing model;[23,24] it describes, in a similar[26] Wigner-like[33] fashion, the "crossed" $s \to p$ and $p \to s$ channel ratio. Specifically,

$$\frac{\chi_{1,2}^2}{\chi_{1,0}^2} = A_1^2\varepsilon^2, \quad \frac{\chi_{0,1}^2}{\chi_{1,0}^2} = B_1\varepsilon. \tag{34}$$

B. Application to new cases

A similar approach can be applied to any of the new mixing cases discussed in Sec. II. First, the definitions of A_1 and

B_1 in Eq. (34) must be generalized to any values of $l \geq 1$:

$$\frac{\chi^2_{l,l+1}}{\chi^2_{l,l-1}} = A_l^2\varepsilon^2, \quad \frac{\chi^2_{l-1,l}}{\chi^2_{l,l-1}} = B_l\varepsilon. \tag{35}$$

Since these definitions follow the original approximation of Hanstorp *et al.*,[26] we shall refer to A_l and B_l as the Hanstorp coefficients. Using these definitions, it is convenient to redefine the Cooper-Zare numerator and denominator expressions in Eq. (23) in the following forms:

$$\begin{aligned} v_l &= \chi^2_{l,l-1}V_l, \\ w_l &= \chi^2_{l,l-1}W_l, \end{aligned} \tag{36}$$

where

$$\begin{aligned} V_l &= \frac{l(l-1)+(l+1)(l+2)A_l^2\varepsilon^2-6l(l+1)A_l\varepsilon\cos\delta_{l+1,l-1}}{2l+1}, \\ W_l &= l+(l+1)A_l^2\varepsilon^2, \end{aligned} \tag{37}$$

are the respective numerator and denominator of Eq. (32),[26] defined in a manner consistent with the definitions of v_l and w_l in Eq. (23).

We now consider a particularly important class of mixing cases, applicable to any sequential binary mixing of the $(l-1)$ and l components of the initial state (e.g., *s-p*, *p-d*, etc.), so that $\gamma_{l-1} + \gamma_l = 1$. Substituting the definitions in Eqs. (36) and (37), into the general mixing formula, as given by Eq. (26), the anisotropy parameter for photodetachment from an $(l-1, l)$ mixed state is expressed as

$$\begin{aligned} \beta_{l-1,l} &= \frac{(1-\gamma_l)v_{l-1}+\gamma_l v_l}{(1-\gamma_l)w_{l-1}+\gamma_l w_l} \\ &= \frac{(1-\gamma_l)\chi^2_{l-1,l-2}V_{l-1}+\gamma_l\chi^2_{l,l-1}V_l}{(1-\gamma_l)\chi^2_{l-1,l-2}W_{l-1}+\gamma_l\chi^2_{l,l-1}W_l}, \\ \beta_{l-1,l}(\varepsilon) &= \frac{(1-\gamma_l)B_l\varepsilon V_{l-1}+\gamma_l A^2_{l-1}\varepsilon^2 V_l}{(1-\gamma_l)B_l\varepsilon W_{l-1}+\gamma_l A^2_{l-1}\varepsilon^2 W_l}. \end{aligned} \tag{38}$$

Equation (38) gives an explicit eKE-dependence of the anisotropy parameter for any sequential binary mixing case $(l-1, l)$. For $l = 1$, Eq. (38) reduces to the familiar *s-p* mixing formula, Eq. (33).[23,24] Although the A_0 coefficient is not defined, it formally cancels out upon the substitution of Eq. (37) into Eq. (38) with $l = 1$.

The next sequential binary case corresponds to the detachment from a mixed *p-d* state. It is described by Eq. (38) with $l = 2$, which gives

$$\beta_{pd}(\varepsilon) = \frac{(1-\gamma_d)B_2\varepsilon\left(2A_1^2\varepsilon^2-4A_1\varepsilon\cos\delta_{2,0}\right)+\gamma_d A_1^2\varepsilon^2\left(2+12A_2^2\varepsilon^2-36A_2\varepsilon\cos\delta_{3,1}\right)/5}{(1-\gamma_d)B_2\varepsilon\left(1+2A_1^2\varepsilon^2\right)+\gamma_d A_1^2\varepsilon^2\left(2+3A_2^2\varepsilon^2\right)}. \tag{39}$$

An example application of the *p-d* mixing formalism in the form of Eq. (39) is demonstrated in Sec. IV.

C. Examples of binary mixing curves

As discussed previously,[3,24] the *s-p* mixing equation with the Hanstorp coefficients, Eq. (33), can be rearranged as follows:

$$\beta_{sp}(\varepsilon) = \frac{2Z_1(A_1\varepsilon)+2(A_1\varepsilon)^2-4(A_1\varepsilon)\cos\delta_{2,0}}{Z_1(A_1\varepsilon)+1+2(A_1\varepsilon)^2}, \tag{40}$$

where Z_1 is a specific $(l = 1)$ case of the composite mixing parameter Z_l, defined as

$$Z_l = \frac{1-\gamma_l}{\gamma_l}\frac{B_l}{A_l}. \tag{41}$$

Neglecting $\delta_{2,0}$ and staying aware of other model constraints, Z_1 can be said to reflect both the physics and chemistry of a mixed *s-p* photodetachment process, by combining the relative channel cross-sections (via A_1 and B_1) with the character of the parent MO (via $\gamma_1 \equiv \gamma_p$).[24] Furthermore, Eq. (40) reveals that for a given value of Z_1, β_{sp} is a unique function of $A_1\varepsilon$. Hence, if the energy scale is normalized with regard of the "size" of the initial orbital (as determined by A_1),[3,26] the anisotropy trend is completely determined by Z_1. This is illustrated in Figure 1, where the anisotropy parameter, per Eq. (40), is plotted versus $A_1\varepsilon$ for different values of Z_1, ranging from $Z_1 = 0$ (pure *p* orbital limit) to $Z_1 = \infty$ (pure *s* limit).

Figure 1 is a complete summary of the mixed *s-p* model.[3,23] It shows that the mixed *s-p* anisotropy trends exhibit a broad variation from the pure *s* limit to the qualitatively different pure *p* limit, depending on the character of the detachment orbital. In particular, even small deviations from the pure *s* limit (e.g., a solvation-induced polarization of an *s* orbital)[23] are predicted to have a large effect on the photodetachment anisotropy. It is for this reason that PADs can be used as a sensitive probe of *s-p* hybridization.[34]

The *p-d* mixing case is notably different. Using the composite *p-d* mixing parameter Z_2, defined by Eq. (41), Eq. (39) can be re-written in a form analogous to Eq. (40):

$$\beta_{pd}(\varepsilon) = \frac{Z_2[2(A_2\varepsilon)-4(A_2/A_1)\cos\delta_{2,0}]+[2+12(A_2\varepsilon)^2-36(A_2\varepsilon)\cos\delta_{3,1}]/5}{Z_2(A_2\varepsilon)^{-1}[(A_2/A_1)^2+2(A_2\varepsilon)^2]+[2+3(A_2\varepsilon)^2]}. \tag{42}$$

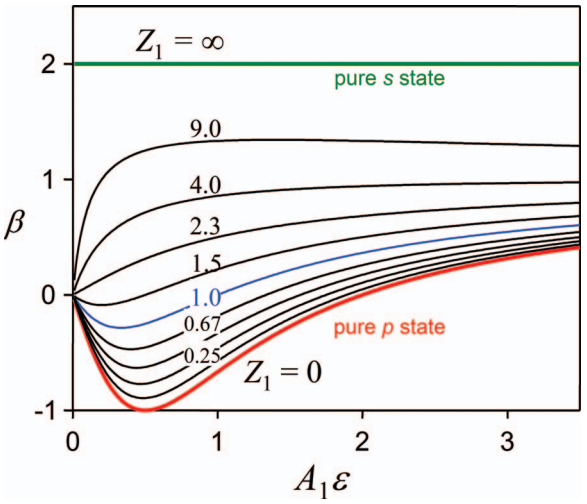

FIG. 1. The electron kinetic energy dependence of the anisotropy parameter for photodetachment from mixed *s*-*p* states, as given by Eq. (40), for different values of Z_1 [defined by Eq. (41)]. All mixing curves shown assume no phase shift ($\delta_{2,0} = 0$). The horizontal axis ($A_1\varepsilon$) corresponds to eKE (ε) normalized for the "size" of the *p* component of the initial state, as expressed by the Hanstorp coefficient A_1. For example, if $A_1 = 1$ eV^{-1}, the axis corresponds to eKE in units of eV. The blue curve corresponds to $Z_1 = 1$. The green and red curves correspond to the respective pure *s* ($Z_1 = \infty$) and pure *p* ($Z_1 = 0$) limiting cases of the mixed *s*-*p* model and coincide exactly with the predictions of the Cooper-Zare central-potential model [Eq. (32)] for $l = 0$ and $l = 1$.

In contrast to *s*-*p* mixing, this equation cannot be summarized in a single graph of β_{pd} vs. $A_2\varepsilon$ for different Z_2 values, because of the additional Hanstorp coefficient, A_1, present in the formula. To illustrate the anisotropy trends, in Figure 2 several β_{pd} curves for varying Z_2 values are plotted vs. $A_2\varepsilon$, all assuming (arbitrarily) $A_1 = 2A_2$. While the appearance of the graph will change with A_1, the key point remains clear, as illuminated by the limited representation of Eq. (42) in Figure 2: at moderate eKEs, the variation among the different *p*-*d* mixing curves is less striking than in the case of *s*-*p* mixing (Figure 1). This is not surprising, considering that the

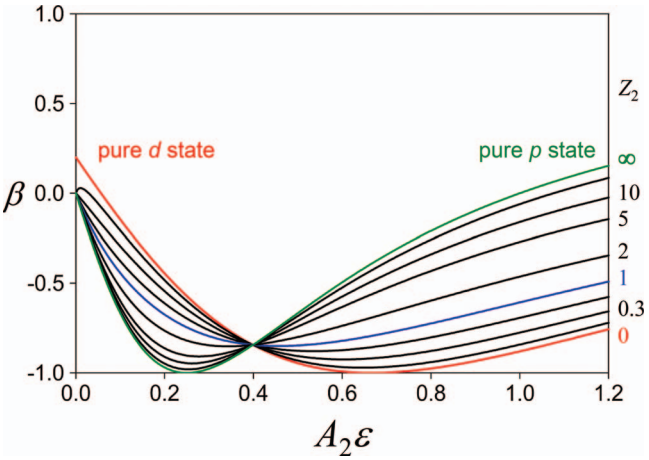

FIG. 2. Energy dependence of the anisotropy parameter for photodetachment from mixed *p*-*d* states, as given by Eq. (42) for different values of Z_2 between 0 (pure *d* state, red curve) and ∞ (pure *p* state, green curve) assuming no phase shifts ($\delta_{2,0} = \delta_{3,1} = 0$) and $A_1 = 2A_2$. See the text and Figure 1 caption for details. The blue curve corresponds to $Z_2 = 1$.

limiting pure *p* and pure *d* curves exhibit qualitatively similar behaviors, both showing a $\beta = -1$ minimum. There is, however, one important distinction between the pure *p* and pure *d* cases, on the one hand, and the mixed *p*-*d* case, on the other. A more-shallow ($\beta > -1$) minimum of the pure *p* or pure *d* Cooper-Zare curves can result only from a non-zero phase-shift between the partial waves. To the contrary, the *p*-*d* mixing curves predict more shallow, in general, minima ($\beta > -1$) even with zero phase-shifts. This is illustrated by the intermediate-Z_2 (e.g., $Z_2 = 1$) curves in Figure 2.

IV. BENCHMARK APPLICATION TO NO$^-$ PHOTODETACHMENT

The photodetachment of NO$^-$, whose HOMO is a $2p\pi^*$ orbital shared between the nitrogen and the oxygen atoms, is a benchmark test for the *p*-*d* mixing case described in Sec. III B. As illustrated in Figure 3, the HOMO (a, left) can be described approximately as a linear combination of a single 3*d* and a single 2*p* type functions, centered halfway between N and O (b).

This description amounts to representing the HOMO in terms of only two basis functions, which may be insufficient for some applications. However, if the functions are chosen with care, the residual contributions of other (larger *l*) components will be small.[35] Since the fractional characters figure as weight factors in Eqs. (21) and (26), minor contributions to Eq. (20) can be neglected, provided the lowest *l* free-electron channels are accounted for.[23] In principle, the model formalism developed in this work, particularly the general mixing formula, Eq. (21), allows for the inclusion of any number of terms in the MO expansion. The two-function approach may be especially useful, if the objective is to capture the essence

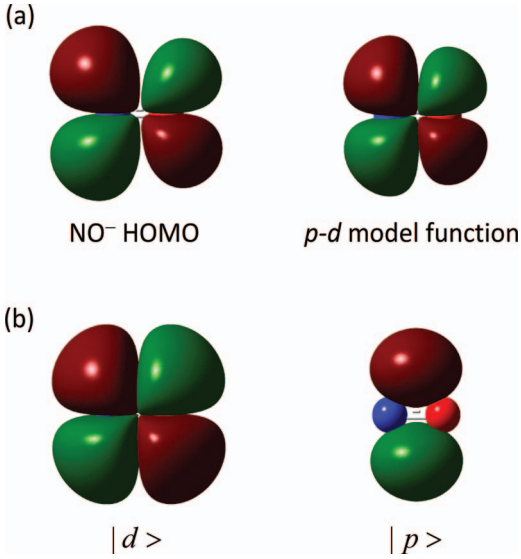

FIG. 3. (a) (Left) NO$^-$ HOMO from CCSD/aug-cc-pVTZ calculations. (Right) the *p*-*d* model function obtained as a least-squares fit of the linear combination [Eq. (18)] of a single 3*d* and a single 2*p* hydrogenic functions, centered halfway between N and O. The optimized fit parameters are: $\gamma_d = 0.985$, $\zeta_{2p} = 1.63$, and $\zeta_{3d} = 5.20$. (b) The individual *d* and *p* components of the model function shown on the right in (a). All plots correspond to an isosurface value of 0.02.

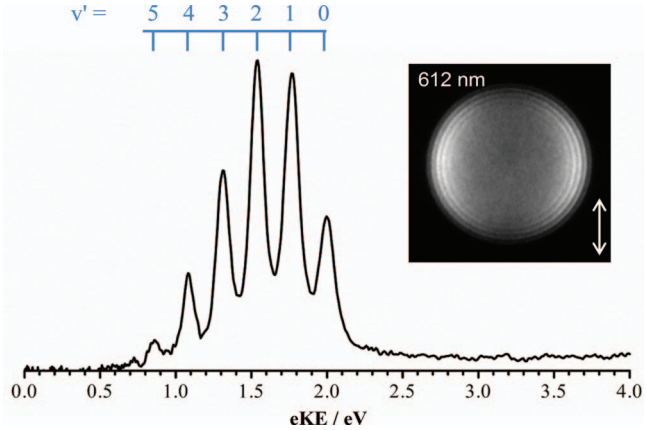

FIG. 4. The NO($X\,^2\Pi$, v′) ← NO^-($X\,^3\Sigma^-$, v″ = 0) photoelectron spectrum obtained at 612 nm. The comb above the spectrum indicates the peak assignments to the vibrational states of neutral NO. The inset on the right shows the corresponding photoelectron image. The double-sided vertical arrow indicates the laser polarization direction.

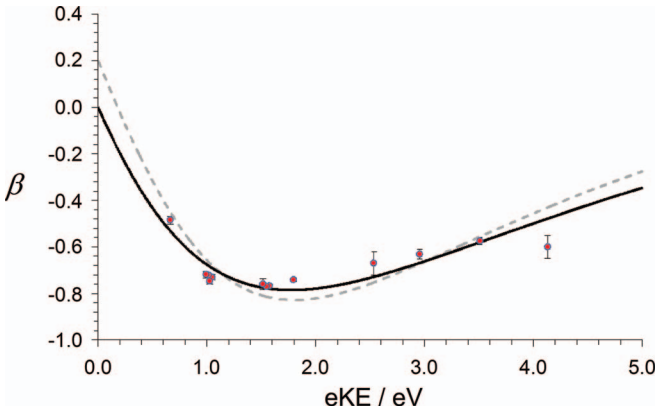

FIG. 5. (Symbols) Experimental energy dependence of the photoelectron anisotropy parameter for the NO($X\,^2\Pi$, v′ = 2) ← NO^-($X\,^3\Sigma^-$, v″ = 0) photodetachment transition at several wavelengths ranging between 1064 nm (the leftmost data point) and 266 nm (the rightmost point). Dashed curve: The least-squares fit to these data using the Cooper-Zare central-potential model [Eq. (32)] with an effective $l = 2$. The optimal fit parameters are: $A_2 = 0.36\ \text{eV}^{-1}$ and $\cos\delta_{3,1} = 0.88$. Solid curve: The *p-d* mixing model prediction using Eq. (39) with $\cos\delta_{2,0} = \cos\delta_{3,1} = 1$, $\gamma_d = 0.985$ (determined from the analysis of the NO^- HOMO), A_1, A_2, and B_2 calculated from ζ_{2p} and ζ_{3d} via Eq. (43), while ζ_{2p} and ζ_{3d} are used as adjustable parameters to fit the curve to the experimental data (optimal values: $\zeta_{2p} = 1.46$ and $\zeta_{3d} = 5.94$).

of the photodetachment process and relate the observables to the dominant character(s) of the parent MO.

The photodetachment of nitric oxide anion has been the subject of many experimental and theoretical studies,[36–38] including several by our group.[34,39–41] The β values were recorded for the NO($X\,^2\Pi$, v′ = 0 – 6) ← NO^-($X\,^3\Sigma^-$, v″ = 0) band at several wavelengths ranging between 1064 and 266 nm. Attempts have been made to fit the experimental $\beta(\varepsilon)$ dependence using the central-potential model, Eq. (32), with an effective $l = 2$. Similar to O_2^-,[12,42] the optimal values of the fit parameters (A_2 and $\delta_{3,1}$) depend on the vibrational state of neutral NO.[39] Here, we consider only the data corresponding, as closely as possible, to vertical photodetachment, as such transitions are most appropriate for comparisons with the model that does not include vibronic effects.

The vibrational state of NO that has the largest Franck-Condon overlap with the ground state of the anion is v′ = 2.[36] This is clearly borne out in the photoelectron imaging data, such as, for example, the 612 nm results for NO^- shown in Figure 4. Both the photoelectron image and the spectrum exhibit a vibrational progression, with v′ = 2 corresponding to the most intense peak. In Figure 5, the experimental β values for the v′ = 2 transitions, obtained in several independent measurements at various wavelengths (from 1064 to 266 nm),[22,34] are plotted versus eKE.

Shown as a dashed curve in Figure 5 is the least-squares fit to these data using the Hanstorp formulation of the Cooper-Zare model, Eq. (32), with an effective $l = 2$, $A_2 = 0.36\ \text{eV}^{-1}$, and $\cos\delta_{3,1} = 0.88$. Although the fit reproduces the observed anisotropy trend quite well, the agreement is not satisfying, because it is based on an unphysical assumption. The NO^- HOMO [Figure 3(a), left] does not have the same symmetry properties as a *d* orbital. The significant phase shift, necessary to reproduce the observed $\beta(\varepsilon)$ trend, points to the flaws inherent in the central potential description. In general, the interaction of the departing electron with the remaining neutral in anion photodetachment is much weaker than the Coulomb attraction in neutral-molecule ionization and the resulting phase shifts tend to be small. Additionally, both the $l = 1$ and $l = 3$ waves turn to zero at the origin ($r = 0$), specifically as a consequence of Eq. (S.18) in the supplementary material.[32] This property decreases the effect of the (weak) core interactions on the individual phases of these waves. The above phase shift, necessary to reproduce the experimental $\beta(\varepsilon)$ dependence using Eq. (32), is inconsistent with these expectations.

The analysis can be improved by describing the lopsided $2p\pi^*$ HOMO of NO^- as a polarized *d* orbital, which is done by adding some *p* character, as illustrated in Figure 3. Hence, we constructed a model *p-d* function, per Eq. (18), as a superposition of one 2*p* and one 3*d* hydrogenic functions centered in the middle of the N–O bond. The spatial extents of these functions are controlled, per Eq. (S.20) in Part B of the supplementary material,[32] by the respective charge parameters, ζ_{2p} and ζ_{3d}. In the present case, these charges do not correspond to any physical atom in NO^-. For this reason, in contrast to our work on carbon-centered *s-p* hybrid orbitals,[24,25,27] ζ_{2p} and ζ_{3d} cannot be assumed to be equal *a priori*.

Overall, the mixed *p-d* model function is defined by three parameters: ζ_{2p}, ζ_{3d}, and the fractional *d* character γ_d. In order to optimize the model function's *d* character, we carried out a least-squares fit (in three spatial dimensions) of the *p-d* model function to the NO^- HOMO determined from CCSD/aug-cc-pVTZ calulations[43] [Figure 3(a), left]. The procedure yielded $\gamma_d = 0.985$, with $\zeta_{2p} = 1.63$ and $\zeta_{3d} = 5.20$. The γ_d value corresponds to only a 1.5% (probability based) *p* character, which translates into a non-trivial 0.12 coefficient for the *p* component in Eq. (18), as $\sqrt{1-\gamma_d} = 0.12$. The resulting model orbital is shown in Figure 3(a), right; it is very similar to the *ab initio* HOMO shown on the left.

The *p-d* mixing formula, Eq. (39), can now be used to model the observed anisotropy trend. The Hanstorp coefficients depend sensitively on the details of the parent orbital

and more work is needed to derive their values in a pure *ab initio* fashion.[24] One feature is clear; however, the A_1, A_2, and B_2 coefficients in Eq. (39) are not entirely independent. Among the three of them, they contain only two degrees of freedom, analogous to the *s-p* mixing case, where the A_1 and B_1 coefficients in Eq. (33) are generally related to each other.[24] If the *p* and *d* components of the model orbital are described by respective 2*p* and 3*d* hydrogenic functions with effective charges ζ_{2p} and ζ_{3d} (as above), the coefficients can be calculated (in atomic units) as

$$A_1 = \frac{16}{\zeta_{2p}^2}, \qquad A_2 = \frac{144}{5\zeta_{3d}^2}, \qquad B_2 = \frac{2^9\zeta_{3d}^7}{5\cdot 3^6\zeta_{2p}^2}. \tag{43}$$

The derivation of these equations is given in Part B of the supplementary material.[32]

Given the above *d* character ($\gamma_d = 0.985$), the anisotropy trend per Eq. (39) is determined by only two independent parameters, ζ_{2p} and ζ_{3d}. We neglect the expected-to-be-small phase shifts (by setting $\cos\delta_{2,0} = \cos\delta_{3,1} = 1$) and fit Eq. (39) to the experimental data in Figure 5. The fit yields the $\beta(\varepsilon)$ dependence plotted in the same figure as a solid curve, with the fit parameter values $\zeta_{2p} = 1.46$ and $\zeta_{3d} = 5.94$. These charges are only slightly different from the respective values obtained above by fitting the *p-d* model orbital to the *ab initio* HOMO ($\zeta_{2p} = 1.63$ and $\zeta_{3d} = 5.20$). The discrepancy is not surprising, given the assumption of the hydrogenic functions to describe the *d* and *p* components of the orbital.

Thus, the *p-d* mixing model prediction reproduces the experimentally observed anisotropy trend quite well. Although the fit is not necessarily "better" (in a mathematical sense) than the single *l* value Cooper-Zare prediction, it is more meaningful, since the underlying model is a more valid representation of the actual physics of the photodetachment process.

V. SUMMARY

A generalized mixing model for molecular-anion PADs has been developed in a form that is, on the one hand, more amendable to experimental applications and, on the other hand, consistent with the Cooper-Zare central-potential formula[6,7] and the previously reported mixed *s-p* model.[23] From the rigorous derivation, a simple empirical form has emerged, allowing for an easy description of the mixing of any number of atomic orbitals of any type. The use of Hanstorp *et al.*'s approximation[26] and the assumption of zero phase-shifts yielded a simplified description of the photoelectron anisotropy parameter as a function of electron kinetic energy in the photodetachment from atomic, molecular, or cluster anion states of any mixed character, which can be compared to the experiment.

While this work addressed *photodetachment* from (in principle) any *anionic* MO, parts of the fundamental formalism in Sec. II may also be useful in describing photoionization processes. However, the following limitations must be considered. First, the Hanstorp approximation is not valid in neutral-molecule ionization. Second, this work took no account of electron scattering from a non-spherical Coulomb potential. The scattering can be neglected in most photodetachment processes, due to the relatively weak and short-range nature of electron-neutral interactions. In neutral-molecule ionization, it will not only affect the partial-wave composition of the free-electron wavefunction but also lead to non-negligible phase-shifts between the partial waves.

The specific photodetachment scenarios considered here within the general model framework include the *s-p* and *p-d* mixing cases. The *s-p* mixing predictions are completely consistent with the previous mixed *s-p* model[23] results. The newly derived *p-d* variant of the model is shown to reproduce the observed anisotropy trend in NO^- photodetachment with physically meaningful parameter values. The successful modeling of this benchmark system further validates both the *p-d* mixing equation and the generalized mixing model from which it was obtained.

ACKNOWLEDGMENTS

This work was supported by the U.S. National Science Foundation (Grant No. CHE-1266152). We thank Dr. Emily R. Grumbling for comments on the paper prior to publication.

[1] K. M. Ervin and W. C. Lineberger, in *Advances in Gas Phase Ion Chemistry*, edited by N. G. Adams and L. M. Babcock (JAI Press, Greenwich, 1992), Vol. 1, p. 121.
[2] K. L. Reid, Annu. Rev. Phys. Chem. **54**, 397 (2003).
[3] A. Sanov, Annu. Rev. Phys. Chem. **65**, 341 (2014).
[4] R. N. Zare, Mol. Photochem. **4**, 1 (1972), http://www.researchgate.net/publication/235207138_Photoejection_Dynamics/file/9c960527c258717d2e.pdf.
[5] H. A. Bethe and E. E. Salpeter, *Quantum Mechanics of One- and Two-Electron Atoms* (Springer-Verlag, Berlin, 1957).
[6] J. Cooper and R. N. Zare, J. Chem. Phys. **48**, 942 (1968).
[7] J. Cooper and R. N. Zare, J. Chem. Phys. **49**, 4252 (1968).
[8] U. Fano and D. Dill, Phys. Rev. A **6**, 185 (1972).
[9] H. Park and R. N. Zare, J. Chem. Phys. **104**, 4554 (1996).
[10] K. J. Reed, A. H. Zimmerman, H. C. Andersen, and J. I. Brauman, J. Chem. Phys. **64**, 1368 (1976).
[11] F. A. Akin, L. K. Schirra, and A. Sanov, J. Phys. Chem. A **110**, 8031 (2006).
[12] M. Van Duzor, F. Mbaiwa, J. Wei, T. Singh, R. Mabbs, A. Sanov, S. J. Cavanagh, S. T. Gibson, B. R. Lewis, and J. R. Gascooke, J. Chem. Phys. **133**, 174311 (2010).
[13] D. J. Goebbert, Chem. Phys. Lett. **551**, 19 (2012).
[14] B. Bandyopadhyay, C. J. M. Pruitt, and D. J. Goebbert, J. Chem. Phys. **138**, 201101 (2013).
[15] A. Kasdan, E. Herbst, and W. C. Lineberger, Chem. Phys. Lett. **31**, 78 (1975).
[16] B. Ritchie, J. Chem. Phys. **60**, 898 (1974).
[17] B. Ritchie, J. Chem. Phys. **61**, 3279 (1974).
[18] B. Ritchie, J. Chem. Phys. **61**, 3291 (1974).
[19] A. Schweig and W. Thiel, J. Chem. Phys. **60**, 951 (1974).
[20] A. D. Buckingham, B. J. Orr, and J. M. Sichel, Philos. Trans. R. Soc., A **268**, 147 (1970).
[21] J. M. Sichel, Mol. Phys. **18**, 95 (1970).
[22] E. R. Grumbling, Ph.D. dissertation, University of Arizona, 2010.
[23] E. R. Grumbling and A. Sanov, J. Chem. Phys. **135**, 164302 (2011).
[24] A. Sanov, E. R. Grumbling, D. J. Goebbert, and L. M. Culberson, J. Chem. Phys. **138**, 054311 (2013).
[25] L. M. Culberson, C. C. Blackstone, and A. Sanov, J. Phys. Chem. A **117**, 11760 (2013).
[26] D. Hanstorp, C. Bengtsson, and D. J. Larson, Phys. Rev. A **40**, 670 (1989).
[27] L. M. Culberson, C. C. Blackstone, R. Wysocki, and A. Sanov, Phys. Chem. Chem. Phys. **16**, 527 (2014).
[28] E. Grumbling and A. Sanov, J. Chem. Phys. **135**, 164301 (2011).
[29] J. C. Tully, R. S. Berry, and B. J. Dalton, Phys. Rev. **176**, 95 (1968).
[30] C. M. Oana and A. I. Krylov, J. Chem. Phys. **127**, 234106 (2007).

[31]C. M. Oana and A. I. Krylov, J. Chem. Phys. **131**, 124114 (2009).
[32]See supplementary material at http://dx.doi.org/10.1063/1.4896241 for the following additional information. Part A: Derivation of the $\theta = 0$ and $\theta = \pi/2$ differential cross-sections in the specific cases of photodetachment from *s* and *d* orbitals. Part B: Analytical evaluation of the Hanstorp coefficients for the 2*p*-3*d* mixing case.
[33]E. P. Wigner, Phys. Rev. **73**, 1002 (1948).
[34]L. M. Culberson, Ph.D. dissertation, University of Arizona, 2013.
[35]For example, the analysis of the 3sσ orbital of the A $^2\Sigma^+$ Rydberg state of NO by H. Rudolph and V. McKoy [J. Chem. Phys. **91**, 2235 (1989)] indicated a dominant *s* (94%) and *d* (5.5%) character, with all other *l* contributions accounting for significantly less than 1%.
[36]M. W. Siegel, R. A. Bennett, R. J. Celotta, J. L. Hall, and J. Levine, Phys. Rev. A **6**, 607 (1972).
[37]M. M. Maricq, N. A. Tanguay, J. C. O'Brien, S. M. Rodday, and E. Rinden, J. Chem. Phys. **90**, 3136 (1989).
[38]M. C. McCarthy, J. W. R. Allington, and K. S. Griffith, Chem. Phys. Lett. **289**, 156 (1998).
[39]L. Velarde, T. Habteyes, E. R. Grumbling, K. Pichugin, and A. Sanov, J. Chem. Phys. **127**, 084302 (2007).
[40]E. R. Grumbling, K. Pichugin, L. Velarde, and A. Sanov, J. Phys. Chem. A **114**, 1367 (2010).
[41]E. R. Grumbling, R. Mabbs, and A. Sanov, J. Chem. Educ. **88**, 1515 (2011).
[42]R. Mabbs, F. Mbaiwa, J. Wei, M. Van Duzor, S. T. Gibson, S. J. Cavanagh, and B. R. Lewis, Phys. Rev. A **82**, 011401 (2010).
[43]M. J. Frisch, G. W. Trucks, H. B. Schlegel *et al.*, Gaussian 09, Revision A.1, Gaussian, Inc., Wallingford, CT, 2009.